

Electron transmission through a steel capillary

J.B. Maljković^a, D. Borka^b, M. Lj. Ranković^a, B.P. Marinković^{a,*}, A.R. Milosavljević^c, C. Lemell^d, K. Tókési^e

^a Institute of Physics Belgrade, University of Belgrade, Pregrevica 118, 11080 Belgrade, Serbia

^b Atomic Physics Laboratory (O40), Vinča Institute of Nuclear Sciences, University of Belgrade, P.O. Box 522, 11001 Belgrade, Serbia

^c Synchrotron SOLEIL, L'orme des Merisiers, Saint-Aubin – BP48, 91192 GIF-sur-Yvette Cedex, France

^d Institute for Theoretical Physics, Vienna University of Technology, Wiedner Hauptstraße 8-10, A-1040 Vienna, Austria

^e Institute for Nuclear Research, Hungarian Academy of Sciences (ATOMKI), H-4026 Debrecen, 4026 Debrecen Bem tér 18/c, Hungary

ARTICLE INFO

Keywords:

Electron scattering from surfaces
Capillary transmission
Metallic capillary
Energy loss

ABSTRACT

The transmission of low-energy electrons through a macroscopic steel capillary has been investigated both experimentally and theoretically. The length of the steel capillary was $L = 19.5$ mm and the inner diameter was $d = 0.9$ mm. The kinetic energy distribution of electrons transmitted through the steel capillary was recorded for a tilt angle of $\psi = 2.6^\circ$ of the incident electron beam with respect to the capillary axis. Accompanying simulations based on classical transport theory reproduce the experimental data to a high degree of agreement. Transmission for other tilt angles has also been simulated to investigate the influence of the tilt angle on the guiding efficiency.

1. Introduction

The understanding and interpretation of electron spectra back-scattered from solid surfaces is important for many technical applications, e.g., for surface characterization and diagnostics to assess material damage and surface modification [1–4]. Additionally, analysis of particles scattered off solid surfaces allows for studying the scattering process itself.

With the advent of capillary targets [5,6] the change of the internal state of the (ionic) projectiles due to the close interaction with the inner capillary wall have become topics of research, since 2002 the redirection of charged particles by nanocapillary targets (see [7,8] and references therein) was investigated in detail.

In our experiment we study electrons escaping macroscopic metallic capillaries after (multiple) impact on the inner wall of the target. Deflection of incident electrons along the capillary axis is accompanied by both elastic and inelastic scattering events and the production of secondary electrons with considerable energy loss of the projectile [9–12]. Clearly, an experimental distinction between transmitted primary particles and secondary electrons generated in inelastic scattering events remains impossible and requires extensive simulations of the transmission process [13–15].

In this work we study the transmission of 150 eV electrons through a macroscopic steel capillary and model the experiment based on classical transport theory [16–19]. The theoretical spectra are presented in

the energy range between 60 eV and 150 eV. For smaller electron energies calculated cross sections become unreliable.

2. Experiment

The experiment was performed on the electron spectrometer UGRA (Institute of Physics Belgrade) which has been modified to allow for mounting of a capillary target [12] instead of a gas needle. The experimental set-up is shown in Fig. 1.

The system consists of a rotatable electron gun, steel capillary, 4-electrode lens, double cylindrical mirror energy analyzer (DCMA), 3-electrode lens, channeltron as a detector and a Faraday cup for obtaining the incident electron beam profile. All components are electrically shielded and enclosed in a vacuum chamber which is magnetically shielded with two layers of μ metal. The working pressure in the experimental chamber during the measurements was about 7×10^{-7} mbar. The electron energy resolution of the system is about 0.7 eV at full width half maximum. The electron gun produces a well collimated electron beam which is directed on the capillary target.

To align the experimental components and to measure the electron beam profile, a Faraday cup was mounted on X – Y manipulator as indicated in Fig. 2. After optimizing and focusing the electron optics for 150 eV energy, the electron beam profile was measured by recording the current in the Faraday cup as a function of the rotation angle Θ_{relative} within the range of about $\pm 4^\circ$ relative to the Faraday cup axis. The

* Corresponding author.

E-mail address: bratislav.marinkovic@ipb.ac.rs (B.P. Marinković).

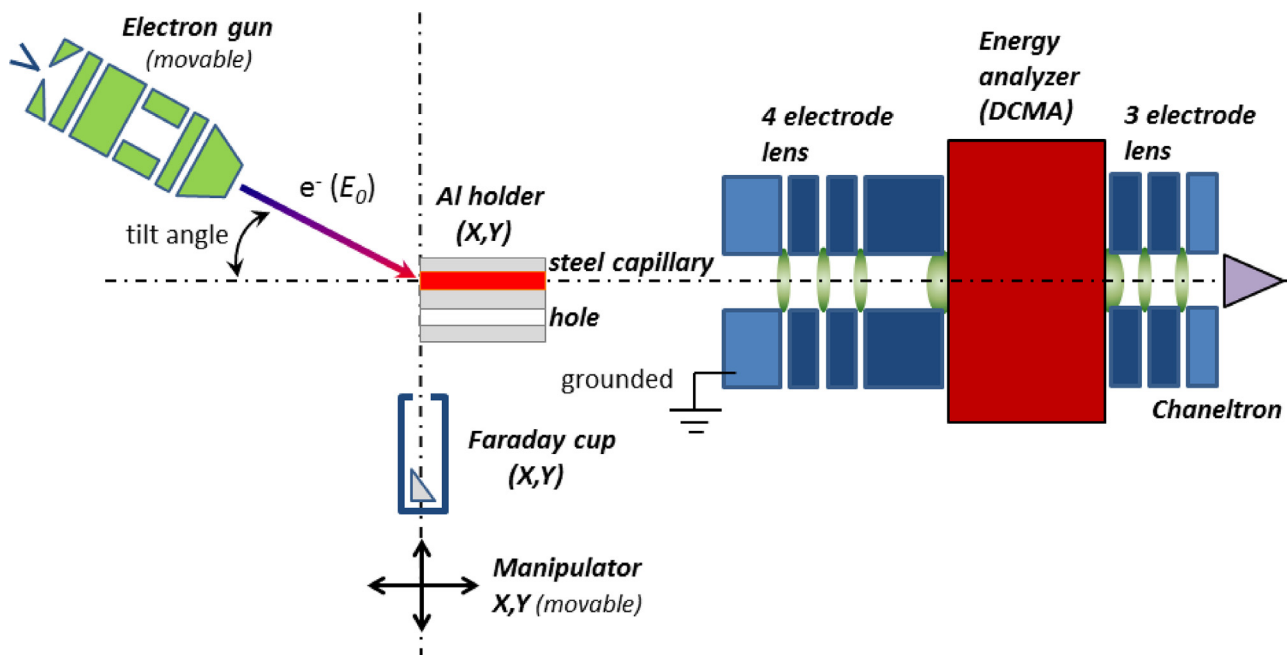


Fig. 1. The experimental set-up UGRA with the movable electron gun, stainless steel capillary, manipulator and double cylindrical mirror energy analyzer with a detector. The analyzer optics and detector are fixed in place. The X–Y manipulator is used to mount either a Faraday cup prior to experiment or an aluminum target holder with the capillary during the experiment.

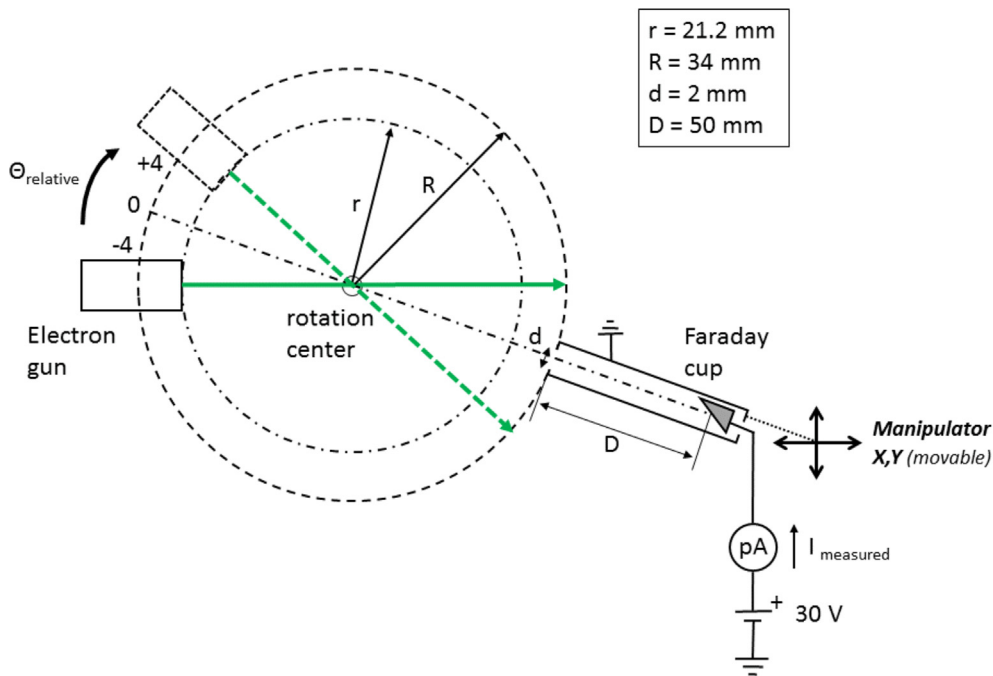


Fig. 2. Schematic representation of setup for measuring the electron beam profile.

Faraday cup was set at a distance of 55 mm from the last electrode of the electron gun.

In order to estimate electron beam width and divergence, a SIMION simulation [20] with the real experimental electrode geometry was performed. In this simulation, starting conditions of electron trajectories were characterized by two parameters, the electron beam width w and the angular divergence da . Initial conditions were uniformly distributed within w and da . The transmission function $T(w, da)$ was simulated for different combinations of w and da until the best agreement between experimental result and simulated data was achieved (Fig. 3). From the comparison we estimated the beam divergence to be

0.3° and a beam diameter of 0.82 mm at the exit of the electron gun.

For the experiment the Faraday cup was replaced by a steel capillary with a diameter of 0.9 mm and a length of 19.5 mm. It has an aspect ratio of 21.7 or, equivalently, a geometric opening angle of 2.6° . The vertical distance between the capillary and a hole was 5.8 mm, while distance between the capillary entrance and last electron gun lens was about 25 mm. The capillary position was adjusted to align with the incident electron beam and the energy analyzer axis. The tilt angle between the incident electron beam and the capillary axis is adjusted by rotating the electron gun with the capillary and analyzer remaining fixed.

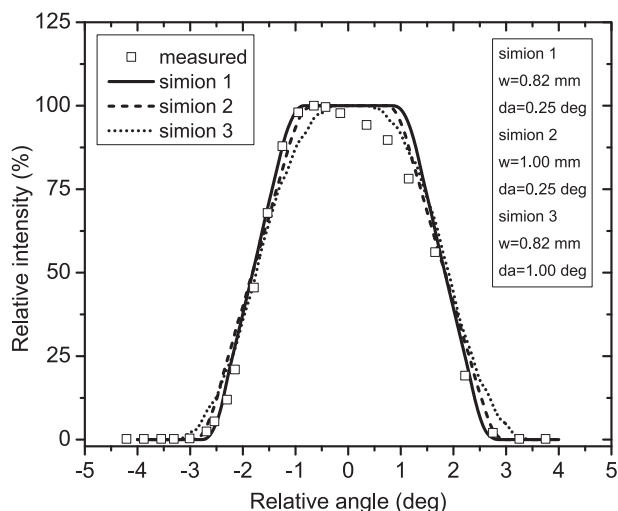


Fig. 3. Measured and simulated electron beam profiles. Symbols: measured profile, lines: SIMION simulations with different parameters; solid line – $w = 0.82$ mm, $da = 0.25^\circ$, dash line – $w = 1.00$ mm, $da = 0.25^\circ$, dot line – $w = 0.82$ mm, $da = 1.0^\circ$.

The system allows for measurements of the transmitted electron current as a function of both the tilt angle and the kinetic energy of electrons escaping the capillary [12]. The electrons transmitted through the steel capillary were energy analyzed by the DCMA operating in constant pass energy mode with counts recorded as a function of a retarding potential. As the transmission of the 4-electrode lens depends on the retarding potential energy distributions of transmitted electrons were corrected according to the transmission function obtained by SIMION. An optimal system alignment was verified by measuring the total transmitted electron current at the inner cylinder of the DCMA.

3. Theory

In our simulation stainless steel is approximated with iron by neglecting any admixtures (Cr, O, C) of unknown quantity. Both elastic and inelastic collisions in Fe are taken into account. Energy dependent cross sections for elastic scattering off Fe atoms modeled with muffin-tin potential were calculated using non-relativistic Schrödinger partial wave analysis [21].

For the description of inelastic scattering cross sections we rely on the dielectric response formalism [22]. Accordingly, the momentum- and energy-loss dependent dielectric function $\epsilon(q, \omega)$ can be approximated by extrapolation of optical data $\text{Im}[-\epsilon(q = 0, \omega)^{-1}]$ into the q - ω plane [23–27]. Then, the bulk and surface energy loss functions are given by $\text{Im}[-\epsilon(q, \omega)^{-1}]$ and $\text{Im}[-\{\epsilon(q, \omega) + 1\}^{-1}]$, respectively [28,29]. The dielectric response of an electron gas has been extensively studied mainly by using the Lindhard type dielectric function [30–35]. The analytical expression given by the Lindhard [36] dielectric function provides a convenient framework for the dielectric properties of Fe. Here, surface and bulk dielectric functions were obtained following Werner et al. [37,38] (see Fig. 4).

Within the capillary electrons follow straight line trajectories. Upon impact on the inner wall of the capillary projectiles undergo a sequence of stochastic scattering events determined by the elastic and inelastic mean free paths. If an electron eventually reescapes from the inner capillary surface the next impact point on the opposite side of the capillary or its escape point from the capillary is calculated. In case of an inelastic scattering event a secondary electron is created with a kinetic energy equal to the energy lost by the primary particle. The initial direction of the secondary electron is chosen randomly from 4π . If its initial kinetic energy is larger than 60 eV its trajectory is subsequently followed as well.

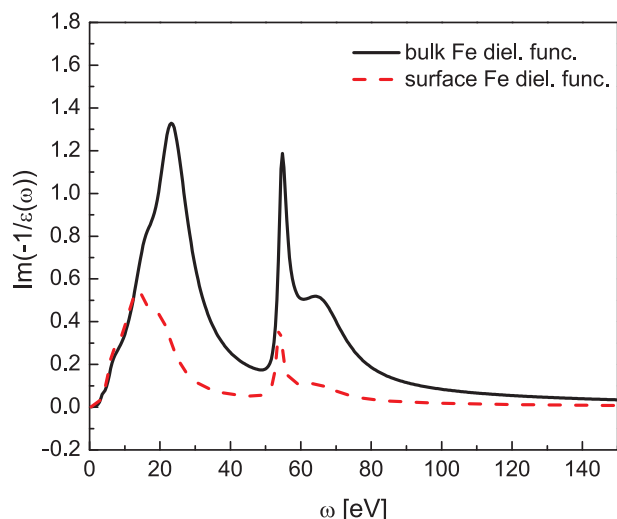


Fig. 4. Bulk (thick solid black line) and surface (thin dashed red line) dielectric functions of Fe [37]. (For interpretation of the references to colour in this figure legend, the reader is referred to the web version of this article.)

4. Results and discussion

In our experiment we selected the smallest angle for which all projectiles have to interact with the inner wall of the capillary, i.e., an angle slightly larger than the geometric opening angle of the capillary. With the linear dimensions of our target capillary (diameter $d = 0.9$ mm, length $L = 19.5$ mm) the tilt angle in the experiment was set to $\psi = 2.6^\circ$. Geometrically, the dominant fraction of electrons are expected to hit the inner surface of the capillary only once. Assuming specular reflection conditions and accounting for a beam divergence of 0.3° more than 75% are expected to undergo only one impact event, another $\sim 20\%$ two impact events (Fig. 5).

From the general shape of the surface and bulk dielectric loss functions (rather broad and featureless functions, Fig. 4) and the small number of impact events we expect the energy distribution of

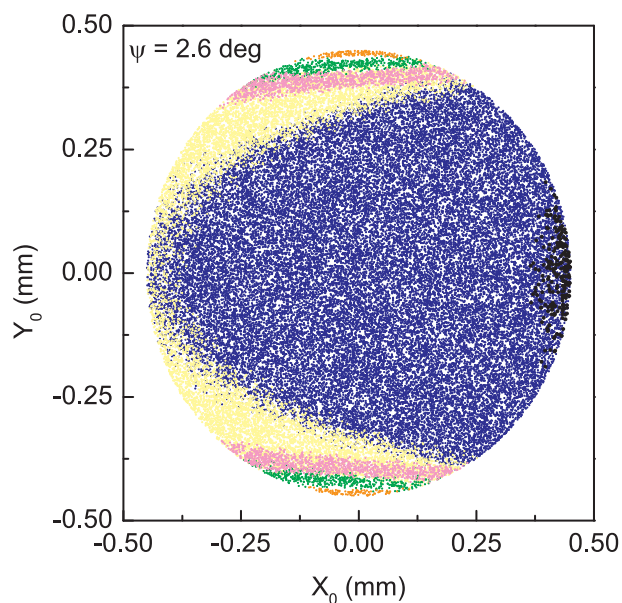


Fig. 5. Trajectories starting from randomly selected positions on the entrance plane under an incidence angle of $2.6 \pm 0.3^\circ$ with respect to the capillary axis are calculated assuming specular reflection upon impact on the inner capillary wall. The number of scattering events is shown in color (0: black 1: blue, 2: yellow, 3: green 4: pink, >4: orange). (For interpretation of the references to colour in this figure legend, the reader is referred to the web version of this article.)

transmitted electrons to resemble the usual energy distributions after backscattering from plane solid surfaces: a sharp elastic peak together with a broad distribution of projectiles having lost a considerable fraction of their initial energy. Towards smaller energies the admixture of secondary electrons increases. Fig. 6 shows our experimental results for 150 eV electrons incident on a steel capillary under an incidence angle of 2.6° (symbols). In general, for small incidence angles one would expect the surface excitations to dominate inelastic scattering events and cause smaller energy loss. Here, however, a clear distinction between surface and bulk losses is not visible presumably due to the surface roughness of the inner wall of the capillary target accompanied by deep penetration into the target under an effectively larger incidence angle. Phonon excitations with energy losses less than about 0.1 eV will only appear as a slight broadening of the elastic peak but have not been analyzed in our experiment. The dominant loss peaks with maxima around 20 and 60 eV are the material characteristic energy losses of electrons in inelastic scattering events containing collective excitations (or plasmons) and single electron excitations. Due to the large number of d electrons in Fe the plasmon peak ($\hbar\omega_{pl} \approx 15.3$ eV) is submerged in the broad distribution around 20 eV (shoulder on the low-energy side of the distribution) and, consequently, cannot be singled out in the electron-energy spectrum as a solitary feature.

To identify surface- or bulk-loss channels we have performed simulations allowing only for surface excitations (thin blue line in Fig. 6) and also for bulk excitations only (thick red line in Fig. 6). Neither simulation run succeeds in perfectly reproducing the experimental results. It can, however, be clearly seen that surface excitation contributions are only responsible for a small fraction of inelastic energy losses. As stated above, this points to a large surface roughness shifting the weight from surface to bulk losses. Additionally, only a minority of electrons leave the surface under the angle of incidence as assumed in the specular reflection model. Therefore, trajectories with more than one impact on the surface will feature on average a larger effective impact angle. This becomes evident when comparing Fig. 5 with Fig. 7 which shows again the starting points of trajectories on the entrance plane.

The dominant fraction of transmitted electrons is still scattered only once but a more realistic description of the electron-wall interaction removes the boundaries between regions with different number of impact events due to an effective randomization of the exit angle from the

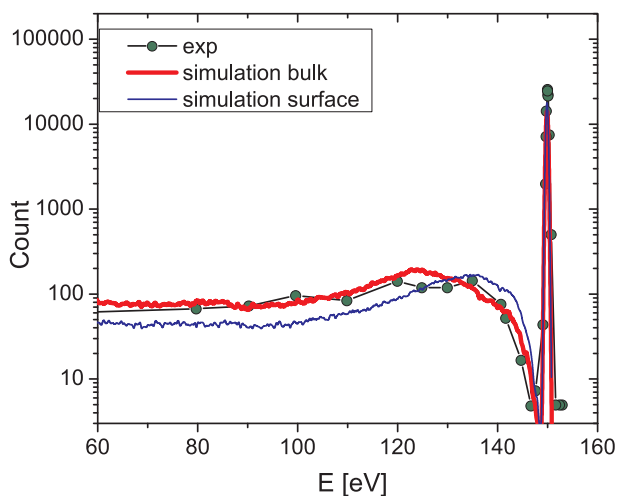


Fig. 6. Comparison between the experimentally obtained kinetic energy spectrum and calculated spectra of electrons escaping the steel tube, for an incident electron energy of 150 eV and electron beam incident angle $\psi = 2.6^\circ$. The simulated spectra have been obtained using the bulk dielectric function (thick red line) and the surface dielectric function (thin blue line) of iron. Experimental data are presented by green circles. (For interpretation of the references to colour in this figure legend, the reader is referred to the web version of this article.)

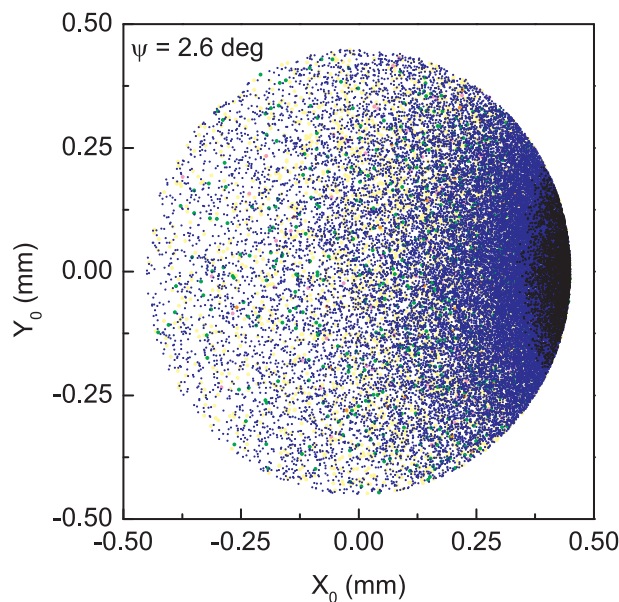


Fig. 7. Same as Fig. 5 but from results of the full simulation for an incidence angle of $\psi = 2.6 \pm 0.3^\circ$. (0: black 1: blue, 2: yellow, 3: green 4: pink, > 4: orange). (For interpretation of the references to colour in this figure legend, the reader is referred to the web version of this article.)

inner capillary wall. This is also related to the neglected reflection at the collective potential of surface atoms [13] active at flat parts of the inner target wall for very grazing incidence angles. Both, the height of the elastic scattering peak in our simulation and the inelastic part of the spectrum is modeled very well.

Increasing the tilt angle in the simulations we have calculated the reduction of the transmission ratio of the capillary, i.e., number of electrons (including secondaries) divided by the number of trajectories started on the entrance plane of the capillary (Fig. 8). The energy and incidence angle of simulated electrons were randomly picked from Gaussian distributions with $E_0 = 150$ eV, $\sigma_E = 0.5$ eV and $\sigma_\psi = 0.3^\circ$, respectively. Only electrons with kinetic energy larger than 50 eV were considered.

Two angular ranges can be discerned: as electrons hitting the surface have only a small probability to re-escape the surface the transmission ratio is for incidence angles smaller than the geometric angle

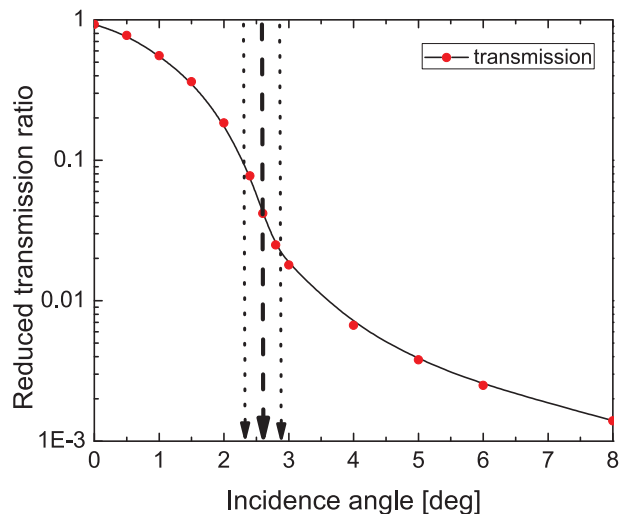


Fig. 8. Reduced transmission ratio as a function of incidence angle. The geometric opening angle is indicated by the dashed line, the beam divergence by the area between the dotted lines. Even at large incidence angles a considerable fraction of electrons are transmitted through the capillary.

dominated by transmission without interaction with the capillary wall. In contrast, for larger angles ($\psi \gtrsim 3^\circ$) every projectile hits the surface at least once thereby considerably reducing the transmission probability. Note, however, that even at larger angles electrons may still be transmitted at the original energy of 150 eV. In our simulation from $\psi = 2.6^\circ$ to $\psi = 5^\circ$ the total transmission probability is reduced by almost an order of magnitude (not considering the increasing intensity of low-energy electrons not included in our simulation).

5. Conclusion

We have presented a joint experimental and theoretical investigation of electrons transmission through a steel capillary with 150 eV primary incident electron energy at $\psi = 2.6^\circ$ which is tilt angle of the capillary. The electron beam divergence was 0.3° . Theoretical spectra were obtained in the energy range between 60 and 150 eV. In the simulation both elastic and inelastic scattering of primary electrons colliding with the inner capillary surface as well as secondary electron emission from the capillary wall were taken into account.

From a comparison of experimental and simulated energy spectra we conclude that the inner wall of our capillary target was very rough suppressing to a large extend specular reflection and interaction with surface loss channels. Instead, best agreement between experiment and theory was found considering only bulk excitations in the simulation of inelastic scattering processes.

Furthermore, we have calculated the transmission ratio of electrons with energies ranging from 60 to 150 eV and found a slowly decreasing transmission function outside the geometric transmission range ($\psi \gtrsim 3^\circ$). While in specular reflection approximation projectiles would have to undergo a large number of impact events for large ψ a realistic description of the surface interaction leads to a randomization of the scattering angle and, consequently, an increased number of trajectories having suffered only few impacts.

Acknowledgments

The work was supported by the Ministry of education, science and technological development of Republic of Serbia under the grants OI 171020 and III 45005. D.B. and C.L. acknowledge support by the bilateral Austrian-Serbian project “Interaction of charged particles with capillaries” number 451-03-01039/2015–09/25, K.T. and C.L. by the *Stiftung Aktion Österreich-Ungarn* under Project No. 96öu9. K.T. acknowledges support by the National Research, Development and Innovation Office (NKFIH) Grant KH 126886. D.B. and K.T. acknowledge support by the European COST Actions CA15107 (MultiComp) and MP1306 (EUSpec).

References

- [1] T.L. Ferrell, P.M. Echenique, *Phys. Rev. Lett.* 55 (1985) 1526.
- [2] H. Cohen, T. Maniv, R. Tenne, Y. Rosenfeld Hacoheh, O. Stephan, C. Colliex, *Phys. Rev. Lett.* 80 (1998) 782.
- [3] F.J. Garcia de Abajo, *Rev. Mod. Phys.* 82 (2010) 209.
- [4] W.S.M. Werner, M. Novák, F. Salvat-Pujol, J. Zemek, P. Jiricek, *Phys. Rev. Lett.* 110 (2013) 086110.
- [5] Y. Yamazaki, S. Ninomiya, F. Koike, H. Masuda, T. Azuma, K.-I. Komaki, K. Kuroki, M. Sekiguchi, *J. Phys. Soc. Jpn.* 65 (1996) 1199.
- [6] S. Ninomiya, Y. Yamazaki, F. Koike, H. Masuda, T. Azuma, K. Komaki, K. Kuroki, M. Sekiguchi, *Phys. Rev. Lett.* 78 (1997) 4557.
- [7] C. Lemell, J. Burgdörfer, F. Aumayr, *Prog. Surf. Sci.* 88 (2013) 237.
- [8] N. Stolterfoht, Y. Yamazaki, *Phys. Rep.* 629 (2016) 1.
- [9] A.R. Milosavljević, Gy. Vákor, Z.D. Pešić, P. Kolarž, D. Šević, B.P. Marinković, S. Mátéfi-Tempfli, M. Mátéfi-Tempfli, L. Piraux, *Phys. Rev. A* 75 (2007) 030901(R).
- [10] S. Das, B.S. Dassanayake, M. Winkworth, J.L. Baran, N. Stolterfoht, J.A. Tanis, *Phys. Rev. A* 76 (2007) 042716.
- [11] B.S. Dassanayake, R.J. Bereczky, S. Das, A. Ayyad, K. Tőkési, J.A. Tanis, *Phys. Rev. A* 83 (2011) 012707.
- [12] A.R. Milosavljević, M. Lj. D. Ranković, J.B. Borka, R.J. Maljković, B.P. Bereczky, K. Tőkési Marinković, *Nucl. Instrum. Methods Phys. Res. B* 354 (2015) 86.
- [13] K. Schiessl, K. Tőkési, B. Solleder, C. Lemell, J. Burgdörfer, *Phys. Rev. Lett.* 102 (2009) 163201.
- [14] D. Borka, K. Tőkési, *Nucl. Instrum. Methods Phys. Res. B* 354 (2015) 112.
- [15] D. Borka, V. Borka Jovanović, C. Lemell, K. Tőkési, *Nucl. Instrum. Methods Phys. Res. B* 406 (2017) 413.
- [16] Z.-J. Ding, R. Shimizu, *Surf. Sci.* 222 (1989) 313.
- [17] R. Shimizu, Y. Kataoka, T. Ikuta, T. Koshikawa, H. Hasimoto, *J. Phys. D: Appl. Phys.* 9 (1976) 101.
- [18] K. Tőkési, D. Varga, L. Kövér, T. Mukoyama, *J. Electron Spectrosc. Relat. Phenom.* 76 (1995) 427.
- [19] K. Tőkési, L. Wirtz, C. Lemell, J. Burgdörfer, *Phys. Rev. A* 64 (2001) 042902.
- [20] D.J. Manura, D.A. Dahl, *SIMION Version 8.0, User Manual*, Scientific Instruments Services Inc, 2007.
- [21] F. Salvat, R. Mayol, *Comput. Phys. Commun.* 74 (1993) 358.
- [22] D. Pines, *Elementary Excitations in Solids*, Benjamin, New York, 1964, p. 127.
- [23] H. Ritchie, *Phys. Rev.* 106 (5) (1957) 874.
- [24] H. Ritchie, A.L. Marusak, *Surf. Sci.* 4 (1966) 234.
- [25] A.G. Eguiluz, D.A. Campbell, *Phys. Rev. B* 31 (1985) 7572.
- [26] J.L. Gervasoni, F. Yubero, *Nucl. Instrum. Methods Phys. Res. B* 182 (2001) 96.
- [27] F. Salvat-Pujol, W.S.M. Werner, *Surf. Interface Anal.* 45 (2013) 873.
- [28] C.J. Powell, *Surf. Sci.* 44 (1974) 29.
- [29] D.R. Penn, *Phys. Rev. B* 35 (1987) 482.
- [30] J.J. Quinn, *Phys. Rev.* 126 (1962) 1453.
- [31] A.L. Fetter, J.D. Walecka, *Quantum Theory of Many-Particle Systems*, McGraw-Hill, New York, 1971, p. 40.
- [32] J.C. Ashley, et al., *Surf. Sci.* 81 (1979) 409.
- [33] C.J. Tung, R.H. Ritchie, *Phys. Rev. B* 16 (1977) 4302.
- [34] H. Raether, *Excitation of Plasmons and Interband Transitions by Electrons*, Springer, Berlin, 1980 ch. 7.
- [35] K. Sturm, *Adv. Phys.* 31 (1982) 1.
- [36] J. Lindhard, K. Dan, *Vidensk. Selsk. Mat. Fys. Medd.* 28 (1954) 1.
- [37] W.S.M. Werner, K. Glantschnig, C. Ambrosch-Draxl, *J. Phys. Chem. Ref. Data* 38 (4) (2009) 1.
- [38] Private communications with W.S.M. Werner.